Genes & Diseases (2015) 2, 337–346

HOSTED BY

Available online at www.sciencedirect.com

ScienceDirect

journal homepage: http://ees.elsevier.com/gendis/default.asp

FULL LENGTH ARTICLE

Chondrogenic priming of human fetal synovium-derived stem cells in an adult stem cell matrix microenvironment

Jingting Li [a,b], Fan He [a,b,c], Ming Pei [a,b,*]

[a] *Stem Cell and Tissue Engineering Laboratory, Department of Orthopaedics, West Virginia University, Morgantown, WV 26506, USA*
[b] *Division of Exercise Physiology, West Virginia University, Morgantown, WV 26506, USA*
[c] *Orthopaedic Institute, Soochow University, Suzhou 215007, China*

Received 5 June 2015; accepted 29 June 2015
Available online 8 July 2015

KEYWORDS
Chondrogenesis;
Decellularized extracellular matrix;
Fetal stem cell;
In vitro microenvironment;
Replicative senescence;
Synovium-derived stem cell

Abstract Cartilage defects are a challenge to treat clinically due to the avascular nature of cartilage. Low immunogenicity and extensive proliferation and multidifferentiation potential make fetal stem cells a promising source for regenerative medicine. In this study, we aimed to determine whether fetal synovium-derived stem cells (FSDSCs) exhibited replicative senescence and whether expansion on decellularized extracellular matrix (dECM) deposited by adult SDSCs (AECM) promoted FSDSCs' chondrogenic potential. FSDSCs from passage 2 and 9 were compared for chondrogenic potential, using Alcian blue staining for sulfated glycosaminoglycans (GAGs), biochemical analysis for DNA and GAG amounts, and real-time PCR for chondrogenic genes including *ACAN* and *COL2A1*. Passage 3 FSDSCs were expanded for one passage on plastic flasks (PL), AECM, or dECM deposited by fetal SDSCs (FECM). During expansion, cell proliferation was evaluated using flow cytometry for proliferation index, stem cell surface markers, and resistance to hydrogen peroxide. During chondrogenic induction, expanded FSDSCs were evaluated for tri-lineage differentiation capacity. We found that cell expansion enhanced FSDSCs' chondrogenic potential at least up to passage 9. Expansion on dECMs promoted FSDSCs' proliferative and survival capacity and adipogenic differentiation but not osteogenic capacity. AECM-primed FSDSCs exhibited an enhanced chondrogenic potential.
Copyright © 2015, Chongqing Medical University. Production and hosting by Elsevier B.V. This is an open access article under the CC BY-NC-ND license (http://creativecommons.org/licenses/by-nc-nd/4.0/).

* *Corresponding author*. Stem Cell and Tissue Engineering Laboratory, Department of Orthopaedics, West Virginia University, PO Box 9196, One Medical Center Drive, Morgantown, WV 26506-9196, USA. Tel.: +1 304 293 1072; fax: +1 304 293 7070.
E-mail address: mpei@hsc.wvu.edu (M. Pei).
Peer review under responsibility of Chongqing Medical University.

http://dx.doi.org/10.1016/j.gendis.2015.06.004
2352-3042/Copyright © 2015, Chongqing Medical University. Production and hosting by Elsevier B.V. This is an open access article under the CC BY-NC-ND license (http://creativecommons.org/licenses/by-nc-nd/4.0/).

Introduction

Articular cartilage possesses limited regenerative abilities when insulted with injury or degenerative disease such as osteoarthritis. Autologous chondrocyte implantation (ACI) is an effective procedure in treating articular cartilage defects[1]; however, there are inherent drawbacks of autologous chondrocytes including limited availability and donor site morbidity which challenge the efficacy of this approach.[2] Human adult stem cells isolated from various tissues have been proposed as promising sources for supplementing autologous chondrocytes.[3] Among them, the synovium-derived stem cell (SDSC) has been characterized as a tissue-specific stem cell for chondrogenesis.[4,5] Though having attracted extensive interest and achieved great success in the past few years, unfortunately, the miniscule quantities of adult stem cells and their dramatic loss of self-renewal abilities and accompanying cellular senescence during *ex vivo* expansion have forced researchers to look for additional alternatives.[6]

Fetal stem cells have been discovered in prenatal tissues, such as umbilical cord blood or vein, amniotic fluid, placenta, and Wharton's jelly.[7] Normally discarded as medical waste, these perinatal tissue-derived fetal stem cells seem useful clinically for autologous transplantation for fetuses and newborns, *in utero* transplantation for genetic disorders, and for banking in later stages of life. Fetal stem cells have been applied in clinical transplantation for different indications in various countries since they are less contentious than embryonic stem cells (ESCs).[8–11] More promising, intrauterine transplantation of fetal mesenchymal stem cells (MSCs) has benefited severe osteogenesis imperfecta.[12] Moreover, accumulating evidence suggests that human fetal MSCs from aborted fetuses possess superior proliferation capacity, better intrinsic homing and engraftment, more robust differentiation potential, and lower immunogenicity, as compared to MSCs from perinatal and postnatal sources.[13] Recent studies also showed that human fetal MSCs maintained their karyotypic and epigenetic stability after more than 100 population doublings *in vitro*, making them even more stable than human ESCs.[14,15]

In our earlier report,[16] late stage (passage 9) fetal SDSCs (FSDSCs) were characterized; the chondrogenic potential of FSDSCs was compared after expansion on either conventional plastic flasks (PL) or decellularized extracellular matrix (dECM) deposited by FSDSCs. Our recent work[17] investigated the replicative senescence of adult SDSCs (ASDSCs) resulting from *ex vivo* expansion on PL and the functional rescue of the chondrogenic potential of ASDSCs *via* expansion on dECM deposited by ASDSCs (AECM) and FSDSCs (FECM), particularly by FSDSCs. However, we did not know whether FSDSCs had replicative senescence and whether AECM had advantages over FECM and PL in priming human FSDSCs in their inherent property — chondrogenic potential. In this study, we hypothesized that, different from ASDSCs, FSDSCs did not exhibit replicative senescence and chondrogenic potential of FSDSCs could be boosted by expansion on AECM.

Materials and methods

dECM preparation

Human FSDSCs were obtained from ScienCell™ Research Laboratories (Carlsbad, CA) and ASDSCs were obtained from Asterand (North America Laboratories, Detroit, MI). Both cell types were used to prepare dECMs, termed FECM and AECM, respectively, as described previously.[16–18] Briefly, PL was precoated with 0.2% gelatin (Sigma–Aldrich, St. Louis, MO) at 37 °C for 1 h and seeded with passage 3 SDSCs at 6000 cells per cm^2. After cells reached 90% confluence, 250 μM of L-ascorbic acid phosphate (Wako Chemicals USA Inc., Richmond, VA) was added for 10 days. The deposited matrix was incubated with 0.5% Triton X-100 containing 20 mM ammonium hydroxide at 37 °C for 5 min to remove the cells; they were stored at 4 °C in phosphate-buffered saline (PBS) containing 100 U/mL penicillin, 100 μg/mL streptomycin, and 0.25 μg/mL fungizone until use.

Cell expansion and morphology

PL expanded passage 3 FSDSCs (PL3) were plated at 3000 cells per cm^2 on FECM, AECM, or PL for one passage with growth medium containing alpha-minimum essential medium (αMEM), 10% fetal bovine serum (FBS), 100 U/mL penicillin, 100 μg/mL streptomycin, and 0.25 μg/mL fungizone. Expanded FSDSCs were termed FE4, AE4, and PL4. Cell number was counted in 175 cm^2 flasks ($n = 6$) using a hemocytometer. To observe cell morphology, FE4, AE4, and PL4 were fixed in 4% paraformaldehyde; the cell membrane was labeled with Vybrant® Dil Cell-labeling solution (Life Technologies, Grand Island, NY) and mounted with Prolong® Gold antifade reagent with 4′,6-diamidino-2-phenylindole (DAPI) (Life Technologies). Both FECM and AECM were immunolabeled using monoclonal antibody for type I collagen (Sigma–Aldrich) conjugated with fluorescein isothiocyanate (FITC) and visualized with a Nikon TE2000-S Eclipse inverted microscope (Melville, NY).

Evaluation of cell proliferation and apoptosis and resistance to oxidative stress

Before cell expansion, PL3 cells were labeled with CellVue® Claret (Sigma–Aldrich) at 2×10^{-6} M for 5 min according to the manufacturer's protocol. After 8 days, expanded cells were collected and measured using a BD FACS Calibur™ flow cytometer (dual laser) (BD Biosciences, San Jose, CA). Twenty thousand events of each sample were collected using CellQuest Pro software (BD Biosciences) and cell proliferation index was analyzed by ModFit LT™ version 3.1 (Verity Software House, Topsham, ME).

Apoptosis of expanded cells was detected using Annexin V-FITC Apoptosis Detection Kit (BioVision Inc., Milpitas, CA). Briefly, 2×10^5 detached cells from each group ($n = 3$) were labeled with FITC conjugated annexin V and propidium iodide for 15 min. Samples were measured using FACS Calibur (BD Biosciences) and analyzed using the FCS Express software package (De Novo Software, Los Angeles, CA).

Expanded cells were incubated with 1 mM hydrogen peroxide (H_2O_2) at 37 °C for 1 h. To measure intracellular reactive oxygen species (ROS), cells were incubated with 1 μM 2′,7′-dichlorodihydrofluorescein diacetate (H_2DCFDA) (Life Technologies) for 15 min. The plates were read on a FlUOstar OPTIMA (BMG Labtech Inc., Cary, NC) with an excitation wavelength of 485 nm and emission of 530 nm. Samples were assayed in triplicate.

Evaluation of surface markers during FSDSC expansion

The following primary antibodies were used to detect expanded FSDSC surface immunophenotype profiles: CD29 (abcam, Cambridge, MA), CD90 (BD Pharmingen, San Jose, CA), CD105 (BioLegend, San Diego, CA), the stage-specific embryonic antigen 4 (SSEA4) (BioLegend), integrin β5 (Cell Signaling, Danvers, MA), and isotype-matched IgGs (Beckman Coulter, Fullerton, CA). The secondary antibody was goat anti-mouse IgG (H + L) R-phycoerythrin conjugated (Life Technologies). Samples ($n = 3$) of each 2×10^5 expanded cells were incubated on ice in cold PBS containing 0.1% Chrom-Pure Human IgG whole molecule (Jackson ImmunoResearch Laboratories, West Grove, PA) and 1% NaN_3 (Sigma–Aldrich) for 30 min. The cells were then sequentially incubated in the dark in the primary and secondary antibodies for 30 min. Fluorescence was analyzed by a FACS Calibur (BD Biosciences) using FCS Express software package (De Novo Software).

Effect of evaluation of cell expansion on FSDSC chondrogenic potential

Plastic expanded FSDSCs (3×10^5) from passage 2 and passage 9 were centrifuged at 500 g for 5 min in a 15-mL polypropylene tube to form a pellet. After overnight incubation (day 0), the pellets were cultured in a serum-free chondrogenic medium consisting of high-glucose Dulbecco's modified Eagle's medium (DMEM), 40 μg/mL proline, 100 nM dexamethasone, 100 U/mL penicillin, 100 μg/mL streptomycin, 0.1 mM ascorbic acid-2-phosphate, and 1× ITS™ Premix (BD Biosciences) with the supplementation of 10 ng/mL transforming growth factor β3 (TGF-β3, PeproTech Inc., Rocky Hill, NJ) in a 5% O_2 incubator as long as 14 days. Chondrogenic potential was evaluated using Alcian blue (AB) staining for sulfated glycosaminoglycans (GAGs), biochemical analysis for DNA and GAG amounts, and TaqMan® real-time polymerase chain reaction (PCR) for aggrecan (*ACAN*) and type II collagen (*COL2A1*).

Effect of evaluation of culture substrates on FSDSC chondrogenic potential

Plastic expanded FSDSCs (3×10^5) from passage 3 were centrifuged at 500 g for 5 min in a 15-mL polypropylene tube to form a pellet. After overnight incubation (day 0), the pellets were cultured in a serum-free chondrogenic medium in a 5% O_2 incubator as long as 21 days. The pellets from day 10 were assessed using AB staining for sulfated GAGs and immunohistochemical labeling (IHC) for type II collagen and TaqMan® real-time PCR for *ACAN* and *COL2A1*. The pellets from day 21 were assessed using AB staining for sulfated GAGs and IHC labeling for type II collagen, TaqMan® real-time PCR for *ACAN* and *COL2A1*, biochemical analysis for DNA and GAG amounts, and biomechanical testing for pellet Stiffness and Young's Modulus (YMOD).

Effect of evaluation of culture substrates on FSDSC adipogenic and osteogenic potentials

For adipogenesis, expanded cells on varied substrates were seeded at 10,000 cells/cm^2 and cultured for 21 days in adipogenic medium (growth medium supplemented with 1 mM dexamethasone, 0.5 mM isobutyl-1-methyxanthine, 200 mM indomethacin, and 10 mM insulin). The cultures ($n = 3$) were fixed in 4% paraformaldehyde and stained with a 0.6% (w/v) Oil Red O (ORO) solution (60% isopropanol, 40% water) for 15 min. Intracellular lipid-filled droplet-bound staining was photographed under a Nikon TE300 phase-contrast microscope (Nikon, Tokyo, Japan). Adipogenic marker genes [lipoprotein lipase (*LPL*) and peroxisome proliferator-activated receptor gamma (*PPARG*)] were quantified using TaqMan® real-time PCR.

For osteogenesis, expanded cells ($n = 3$) were seeded at 8000 cells/cm^2 and cultured for 21 days in osteogenic medium (growth medium supplemented with 0.1 mM dexamethasone, 10 mM β-glycerol phosphate, 50 mM ascorbate-2-phosphate, and 0.01 mM 1,25-dihydroxyvitamin D_3) were collected for alkaline phosphatase (ALP) activity assay with a reagent kit (Sigma–Aldrich) by measuring the formation of p-nitrophenol (p-NP) from p-nitrophenyl phosphate following the manufacturer's instructions. p-NP was quantified based on the spectrophotometric absorbance at 405 nm and enzymatic activity was expressed as millimoles of p-NP/min/mg DNA. For evaluation of calcium deposition, induced cells ($n = 3$) were fixed with 70% ice-cold ethanol for 1 h and then incubated in 40 mM Alizarin Red S (ARS) at pH 4.2 for 20 min with agitation. After rinsing, matrix mineral-bound staining was photographed. Quantification of staining was performed by incubating cells with a solution of 10% acetic acid and 20% methanol for 15 min to extract the calcium-chelated ARS stain. Samples were analyzed for absorption at 450 nm, which was normalized to total DNA amount for standardization.

Histology and immunolabeling

Representative pellets ($n = 2$) were fixed in 4% paraformaldehyde at 4 °C overnight, followed by dehydrating in a gradient ethanol series, clearing with xylene, and embedding in paraffin blocks. 5-μm sections were stained with AB staining (counterstained with fast red) for sulfated GAGs. For immunohistochemistry, the sections were immunolabeled with a primary antibody against type II collagen [II-II6B3, Developmental Studies Hybridoma Bank (DSHB), Iowa City, IA], followed by the secondary antibody of biotinylated horse anti-mouse IgG (Vector, Burlingame, CA). Immunoactivity was detected using Vectastain ABC reagent (Vector) with 3,3′-diaminobenzidine as a substrate.

Biochemical analysis for DNA and GAG amount

Representative pellets ($n = 4$) were digested at 60 °C for 4 h with 125 μg/mL papain in PBE buffer (100 mM

phosphate, 10 mM ethylenediaminetetraacetic acid, pH 6.5) containing 10 mM cysteine. To quantify cell density, the amount of DNA in the papain digestion was measured using the QuantiT™ PicoGreen® dsDNA assay kit (Life Technologies) with a CytoFluor® Series 4000 (Applied Biosystems, Foster City, CA). GAG was measured using dimethylmethylene blue dye and a Spectronic™ BioMate™ 3 Spectrophotometer (Thermo Fisher Scientific, Waltham, MA) with bovine chondroitin sulfate (Sigma–Aldrich) as a standard.

TaqMan® real-time PCR

Total RNA was extracted from pellets ($n = 4$) using an RNase-free pestle in TRIzol® (Life Technologies). Two μg of mRNA were used for reverse transcriptase with the High-Capacity cDNA Archive Kit (Applied Biosystems) at 37 °C for 120 min. Chondrogenic marker genes [*ACAN* (Assay ID AIQJAP5) and *COL2A1* (Assay ID Hs00156568_m1)] and adipogenic marker genes [*LPL* (Assay ID Hs00173425_m1) and *PPARG* (Assay ID Hs01115513_m1)] were customized by Applied Biosystems as part of their Custom TaqMan® Gene Expression Assays. Eukaryotic *18S* rRNA (Assay ID HS99999901_s1 ABI) was carried out as the endogenous control gene. Real-time PCR was performed with the iCycler iQ™ Multi Color RT-PCR Detection kit and calculated by computer software (Perkin–Elmer, Wellesley, MA). Relative transcript levels were calculated as $\chi = 2^{-\Delta\Delta Ct}$, in which $\Delta\Delta Ct = \Delta E - \Delta C$, $\Delta E = Ct_{exp} - Ct_{18s}$, and $\Delta C = Ct_{ct1} - Ct_{18s}$.

Biomechanical testing

Representative pellets ($n = 6$) were placed into a reservoir filled with PBS and loaded onto the custom miniature stepper motor driven compression device. This device used a 10 g load cell and a miniature differential variable reluctance transducer (DVRT) for displacement readout. A small preload of 0.0001 N was applied followed by a 10% strain at 1 s duration. From the linear portion of the load displacement curve, the Stiffness and YMOD were calculated for the spherical shaped pellet according to Rodriguez and colleagues.[19]

Statistical analysis

A Mann–Whitney U test and a linear model with contrast analysis were used for pairwise comparison. All statistical analyses were performed with SPSS 13.0 statistical software (SPSS Inc., Chicago, IL). p values less than 0.05 were considered statistically significant.

Results

Cell expansion enhanced FSDSCs' chondrogenic potential

To determine whether cell passaging on plastic flasks would affect expanded cells' chondrogenic potential, human FSDSCs from passage 2 and passage 9 were evaluated after

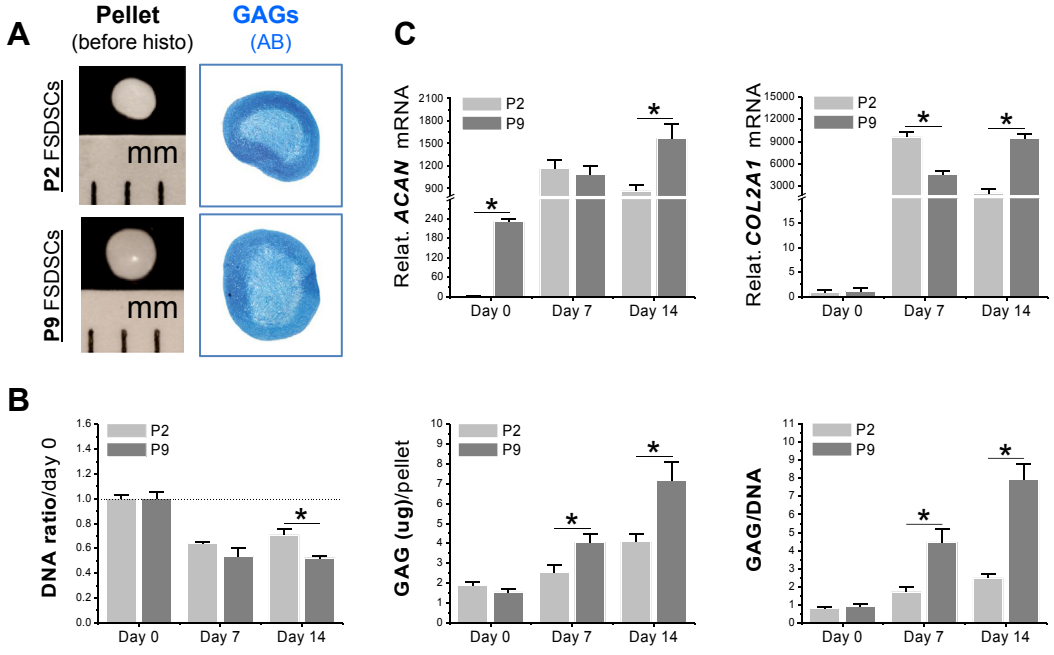

Fig. 1 Later passage FSDSCs exhibited an enhanced chondrogenic potential. Passage 2 (P2) and P9 FSDSCs were chondrogenically induced in a pellet culture system for 14 days. The effect of passaging on FSDSC chondrogenic capacity was evaluated using (A) histology, including pellet size (mm) and Alcian blue staining for sulfated GAGs, (B) biochemical analysis for DNA and GAG contents of pellets with DNA ratio indicating cell viability and a ratio of GAG to DNA indicating chondrogenic index, and (C) real-time PCR for chondrogenic marker gene expression (*ACAN* and *COL2A1*). Data are shown as average ± standard deviation (SD) for $n = 4$. *$p < 0.05$ indicated a statistically significant difference.

14-day chondrogenic induction. The pellets from passage 9 cells were bigger in size with a shiny surface; AB staining showed comparable intensity to those from passage 2 cells (Fig. 1A). Biochemical analysis data showed that, despite a higher DNA ratio (by day 0) in 14-day pellets than those from passage 9 cells, the pellets from passage 2 cells exhibited a lower amount of GAG per pellet and a lower ratio of GAG to DNA at both day 7 and day 14 (Fig. 1B). Real-time PCR data showed that, compared to a continuing increase in passage 9 cells, both *ACAN* and *COL2A1* increased at day 7 but decreased at day 14 in passage 2 cells (Fig. 1C).

dECM expansion promoted FSDSCs' proliferative and survival capacity

To evaluate the proliferative effect exerted by AECM and FECM expansion, human FSDSCs were seeded for one passage on three different substrates: PL, AECM, or FECM. Cells grown on PL exhibited random organization and spindle morphology (red color); in contrast, cells expanded on dECMs were more elongated and well organized by lining up with matrix fibers in which type I collagen was positively detected (initial color was green and merged color was yellow) (Fig. 2A). Six-day-expansion on FECM yielded the highest cell number followed by AECM with PL having the lowest (Fig. 2B). This finding was supported by proliferation index (PI) data, in which AECM expansion yielded a 1.8-fold increase and FECM expansion yielded a 2.5-fold increase compared with PL expansion (Fig. 2C).

Our flow cytometry data showed that expanded FSDSCs from all groups exhibited a similar percentage of apoptotic cells (Fig. 2D). To evaluate cell viability after expansion on these substrates, 1 mM H_2O_2 was applied to measure ROS scavenging capacities in expanded FSDSCs. Both FECM and AECM expanded cells produced about half the ROS compared to PL upon stimulus (Fig. 2E), indicating dECM expanded FSDSCs had higher viability in a harsh environment.

To evaluate the effect of dECM expansion on MSC surface markers of FSDSCs, our flow cytometry data showed that in both AECM and FECM expanded FSDSCs, CD29 and CD90 were down-regulated in median fluorescence intensity (median) with CD105 down-regulated in both median and percentage. Interestingly, SSEA4 was up-regulated in both

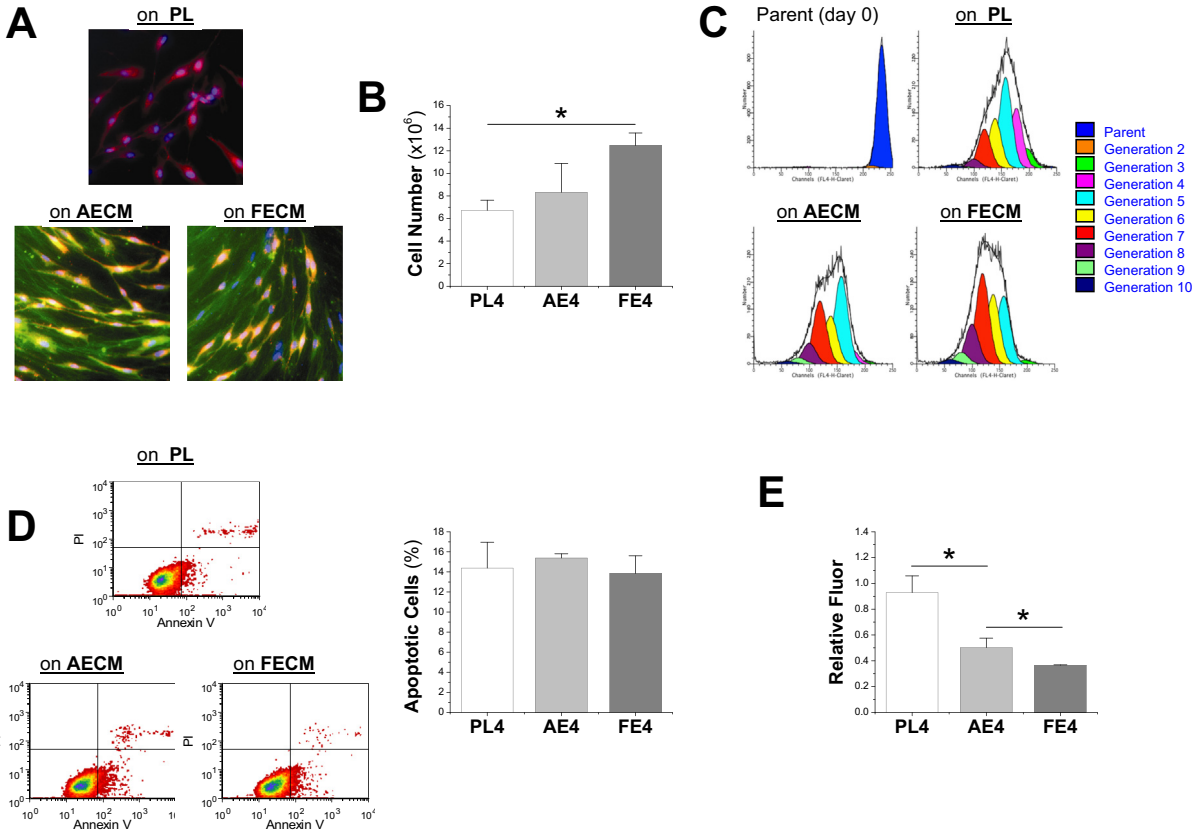

Fig. 2 dECM expanded FSDSCs exhibited an enhanced proliferation and resistance to oxidative stress, especially for cell expansion on FECM. (A) FSDSCs were expanded on three substrates (PL, AECM, and FECM) for one passage; the cell membrane was labeled with Vybrant Dil Cell labeling solution (red) and the nuclei were stained using DAPI (blue), the dECM fibers were immunolabeled for type I collagen (green). (B) Cell number was counted in 175 cm^2 flasks ($n = 6$) using a hemocytometer. (C) Flow cytometry was used to measure the proliferation index of expanded ASDSCs. (D) Flow cytometry was used to measure percentage of apoptotic cells after expansion on the three substrates. (E) Generation of ROS following hydrogen peroxide incubation was evaluated. Relative fluorescence emitted by fluorescent dye 2′,7′-dichlorofluorescein diacetate was measured and is presented as means ± standard deviation (SD) of the mean for $n = 3$. *$p < 0.05$ indicated a statistically significant difference.

percentage and median while integrin β5 was up-regulated only in median (Fig. 3).

AECM primed FSDSCs exhibited an enhanced chondrogenic potential

To determine the priming effects of dECM expansion on FSDSCs' chondrogenic potential, expanded cells were chondrogenically induced for up to 21 days. At the early stage, 10-day pellets from PL3, PL4, and FE4 were similar in size while those from AE4 were slightly bigger; the pellets from dECM expansion were intensely stained with Alcian blue for sulfated GAGs and immunolabeled for type II collagen compared to those from PL expansion (Fig. 4A). Chondrogenic marker gene (*ACAN* and *COL2A1*) expression further revealed that dECM expansion up-regulated chondrogenic genes with AE4 being the highest, followed by FE4 (Fig. 4B). Consistent with the above cell expansion data in Fig. 1C, PL4 cells exhibited a higher level of *ACAN* and *COL2A1* than PL3 cells after 10-day chondrogenic induction (Fig. 4B).

At the later stage, 21-day pellets were evaluated for chondrogenic differentiation and functionality. Similar to the data at day 10, the pellets from PL3, PL4, and FE4 groups were comparable in size; the pellets from dECM expansion, particularly from AE4, were bigger and intensely stained for sulfated GAGs and type II collagen (Fig. 5A). The pellets from AE4 exhibited the highest level of chondrogenic marker genes (*ACAN* and *COL2A1*) followed by those from PL expansion (*ACAN* and *COL2A1*); pellets from the FE4 group had the lowest level (*ACAN* and *COL2A1*) (Fig. 5B). Our biochemistry data showed that, after chondrogenic induction, AECM expansion yielded higher cell viability (DNA% by day 0) though it was not significantly different; AECM expansion yielded the highest GAG amount per pellet, followed by those from FECM expansion with PL expansion having the least with a comparable ratio of GAG to DNA among groups (Fig. 5C). Our functionality data suggested that dECM expansion yielded FSDSC pellets with comparable Stiffness and Young's modulus with those from PL expansion (Fig. 5D).

dECM expanded FSDSCs exhibited an enhanced adipogenic potential rather than osteogenic capacity

To determine the rejuvenation effect of dECM expansion on FSDSC adipogenic and osteogenic potentials, expanded cells were incubated in corresponding lineage induction medium for 21 days. Our adipogenic induction data showed that expanded FSDSCs from varied substrates all stained positive for ORO (Fig. 6A); FE4 exhibited the highest levels of *LPL* and *PPARG* mRNAs followed by AE4 (*LPL*); PL expansion had the lowest levels (Fig. 6B). Our osteogenic induction data showed that expanded FSDSCs from varied substrates all stained positive for ARS (Fig. 6C) and ALP (Fig. 6E). Quantitative assessment for relative ARS density (Fig. 6D) and ALP activity (Fig. 6F) did not show a significant difference between groups.

Discussion

To achieve successful cartilage repair, stem cells for application in cartilage regeneration should be obtained easily, non-invasively, and in sufficient quantities and then transplanted safely and efficiently to a host.[20] Fetal stem cells are a promising source; however, there are limited studies investigating the potential of these sources in cartilage regeneration. Our group was the first to characterize FSDSCs through expression of MSC markers

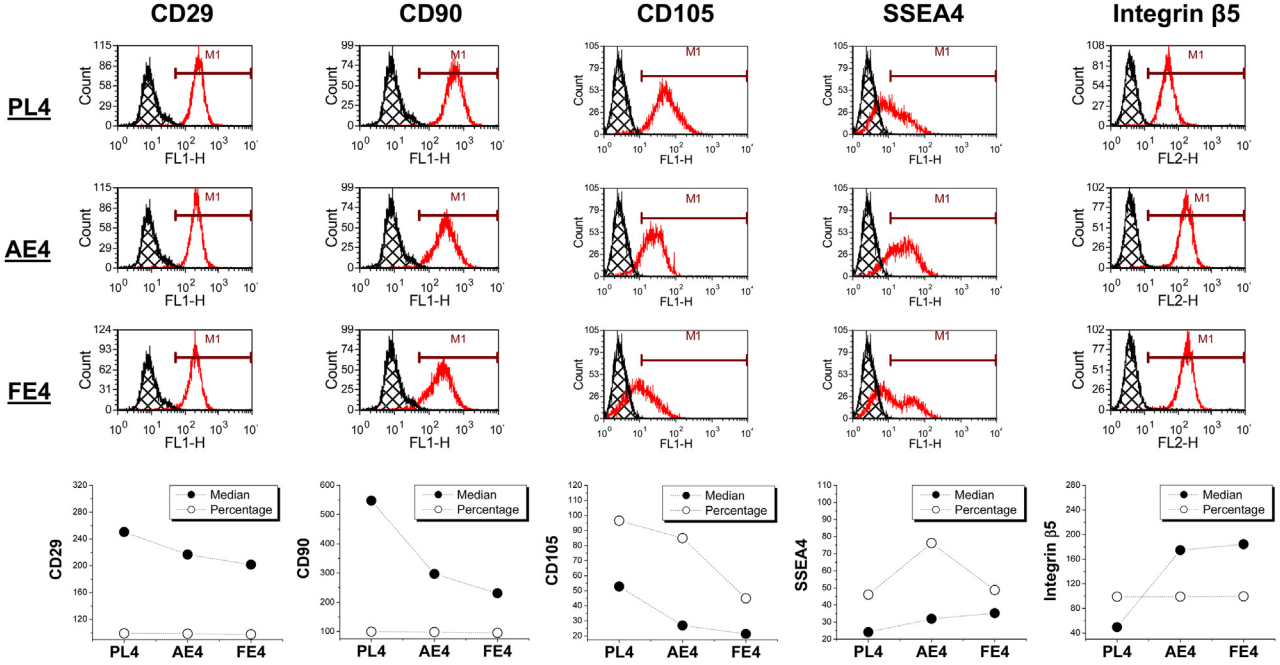

Fig. 3 Flow cytometry was used to measure both percentage and median of MSC surface markers (CD29, CD90, and CD105), SSEA4, and integrin β5 in human FSDSCs after one passage on three substrates (PL, AECM, and FECM).

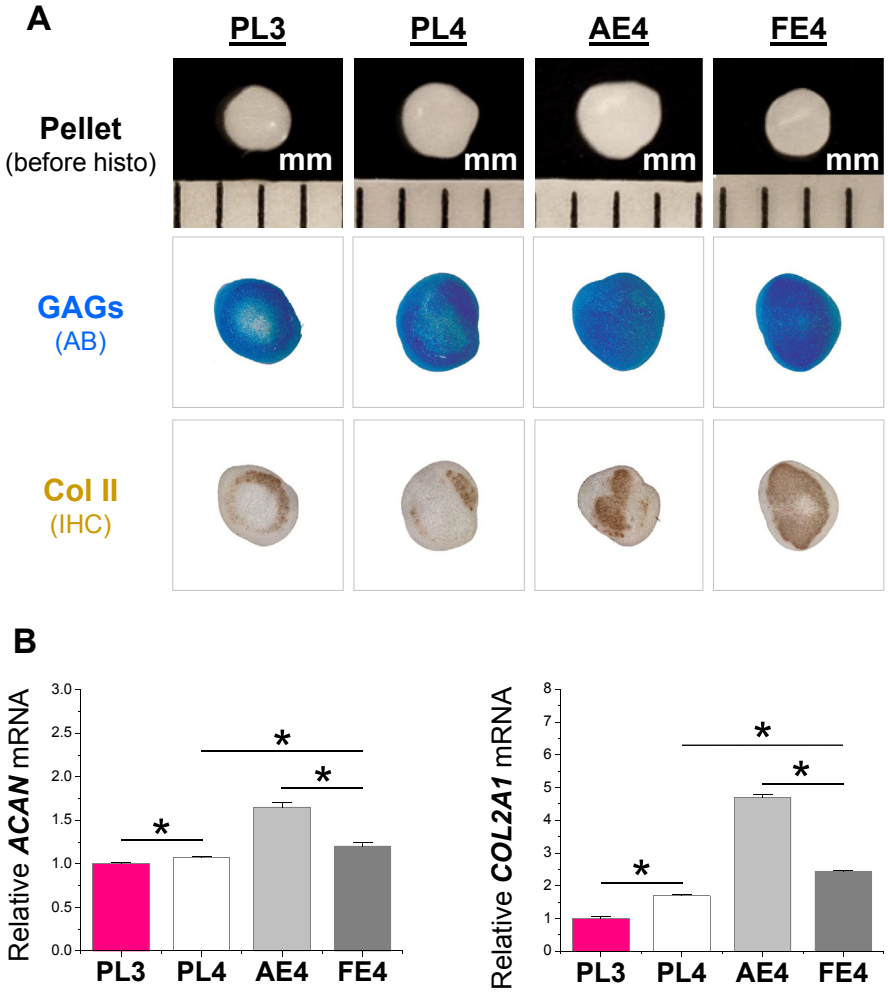

Fig. 4 AECM promoted expanded FSDSCs' early chondrogenic differentiation. PL expanded passage 3 FSDSCs (PL3) were grown on PL, AECM, or FECM for one passage; the expanded cells were PL4, AE4, and FE4. The above four cells were chondrogenically induced in a pellet culture system for 10 days. (A) Before histological staining, pellet size was measured with a scale bar in mm; Alcian blue (AB) was used to stain sulfated GAGs and immunohistochemistry labeling (IHC) was used to detect type II collagen (Col II). (B) Real-time PCR was used to evaluate chondrogenic marker gene expression (*ACAN* and *COL2A1*) in day 10 pellets. Data are shown as average ± standard deviation (SD) for $n = 4$. *$p < 0.05$ indicated a statistically significant difference.

CD90, CD105, CD29, and SSEA4 and multi-lineage differentiation potential.[16] In this study, we found that FSDSCs exhibited an enhanced chondrogenic potential during cell expansion at least up to passage 9. Expansion on dECM promoted FSDSCs' ability in proliferation and resistance to oxidative stress, particularly on FECM, while expansion on AECM promoted FSDSCs' ability in chondrogenic differentiation. Interestingly, expansion on dECM also enhanced FSDSCs' ability in adipogenesis rather than osteogenesis.

Our previous reports showed that adult stem cell passaging on conventional plastic flasks could cause replicative senescence, evidenced by a down-regulation of the ratio of GAG to DNA (chondrogenic index), *ACAN*, and *COL2A1* in porcine SDSCs from passage 3 to 5[21] and in human bone marrow stromal cells (BMSCs) from passage 5 to 8.[22,23] To the best of our knowledge, for the first time, the findings in this study indicated that replicative senescence did not apply to fetal source SDSCs, which exhibited an enhanced chondrogenic capacity after expansion from passage 2 to 9. The discrepancy between fetal and adult SDSCs also existed in their response to dECM. In a recently published parallel study,[17] despite a higher level of GAG amount in each pellet from FSDSCs compared to ASDSCs (38.89 ± 2.59 μg versus 24.60 ± 1.42 μg) after a 21-day chondrogenic induction, FSDSC expansion on either AECM (1.52-fold increase) or FECM (1.38-fold increase) yielded pellets with a lower level of GAG amount per pellet than those from ASDSC expansion (2.78- and 4.42-fold increase, respectively). Consistent with a previous report that fetal BMSCs expressed higher osteogenic genes and deposited a higher level of calcium compared to adult BMSCs in nude mice,[24] this finding suggested that human FSDSCs exhibited higher chondrogenic potential than human ASDSCs despite more sensitivity of ASDSCs to chondrogenic priming from dECM expansion. Interestingly, we found the most chondrogenic capacity was achieved for ASDSCs by expansion on FECM and for FSDSCs by expansion on AECM, indicating that the shortage of "stemness" signals in adult SDSCs could be supplemented by fetal matrix while the shortage of

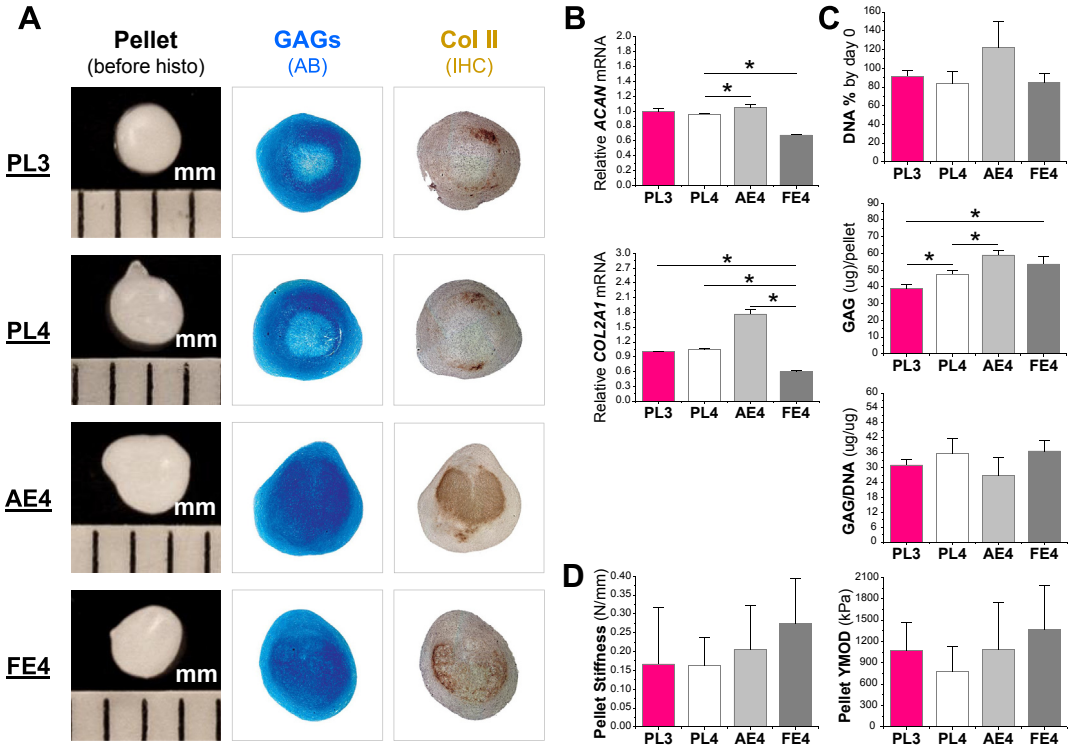

Fig. 5 AECM promoted expanded FSDSCs' later chondrogenic differentiation. PL expanded passage 3 FSDSCs (PL3) were expanded on either PL, AECM, or FECM for one passage; the expanded cells were PL4, AE4, and FE4. The above four cells were chondrogenically induced in a pellet culture system for 21 days. (A) Before histological staining, pellet size was measured with a scale bar in mm; Alcian blue (AB) was used to stain sulfated GAGs and immunohistochemistry labeling (IHC) was used to detect type II collagen (Col II). (B) Real-time PCR was used to evaluate chondrogenic marker gene expression (*ACAN* and *COL2A1*). (C) Biochemical analysis was used for DNA and GAG contents of pellets; cell viability in chondrogenic medium was evaluated using DNA ratio (DNA content at day 21 adjusted by that at day 0); a ratio of GAG to DNA indicated chondrogenic index. (D) Functionality of chondrogenically differentiated pellets was evaluated using Stiffness and Young's modulus. Data are shown as average ± standard deviation (SD) for $n = 4$. *$p < 0.05$ indicated a statistically significant difference.

"differentiation" signals in fetal SDSCs could be boosted by adult matrix.

Decellularized ECM deposited by MSCs has been proven an effective *ex vivo* expansion system for both stem cells[16,21–23,25–27] and primary cells.[28–30] In this study, we found that, despite the inherent proliferative potential that FSDSCs possess, which might be associated with longer telomeres and higher telomerase activity in fetal MSCs,[24] expansion on both dECMs, especially on FECM, increased cell yield and resistance to oxidative stress. Compared to ASDSC expansion in a parallel study,[17] passage 3 FSDSC expansion exhibited a higher level of proliferation index when grown on Plastic (12.6 versus 2.1), AECM (22.7 versus 4.5), or FECM (31.0 versus 5.4). Similar enhancement of adult BMSC *ex vivo* expansion by fetal BMSC ECM was reported by Ng and colleagues.[31]

Although initiation of chondrogenesis of both fetal and adult MSCs was modulated by distinct signaling mechanisms,[32] the fate of MSCs is also affected by the surrounding ECM.[33] For instance, dECM expansion could protect SDSCs from oxidative and senescent insults[16,18]; interaction with ECM from young cells was sufficient to restore aged, senescent cells to an apparently youthful state through induction of both Ku and SIRT1.[34] Our recent parallel study indicated that FECM was better than AECM in promoting cell proliferation and preventing apoptosis, which might be explained by the discrepancy in chemical composition of these two matrices.[17] Our proteomics data showed that FECM had more fibrillin-2, tenascin C, and clusterin than AECM.[17] Despite being largely restricted to developing fetal tissues,[35] enhanced expression of fibrillin-2 and tenascin C has been observed in adults with fibroproliferative conditions, such as wound healing and sclerosis.[36–38] AECM had more biglycan, decorin, dermatopontin, elastin, periostin, thrombospondin-1, and TGF-β1 than FECM.[17] Decorin and biglycan were reported to reduce proliferation of pre-adipocytes, partly by induction of apoptosis.[39] Dermatopontin has been implicated in chondrogenic differentiation.[40,41] Notably, periostin and TGF-β are involved in osteochondrogenesis.[42] Thrombospondin-1 signaling through CD47 inhibits self-renewal by regulating c-Myc and other stem cell transcription factors.[43] The above data showed that, compared with the role of FECM during cell expansion, AECM has more matrix components favoring cell differentiation and apoptosis rather than cell proliferation.

In this study, we also found that dECM expansion enhanced FSDSC adipogenic potential rather than osteogenic capacity. This finding is in line with our parallel study,[17] in which ASDSCs were compared for tri-lineage

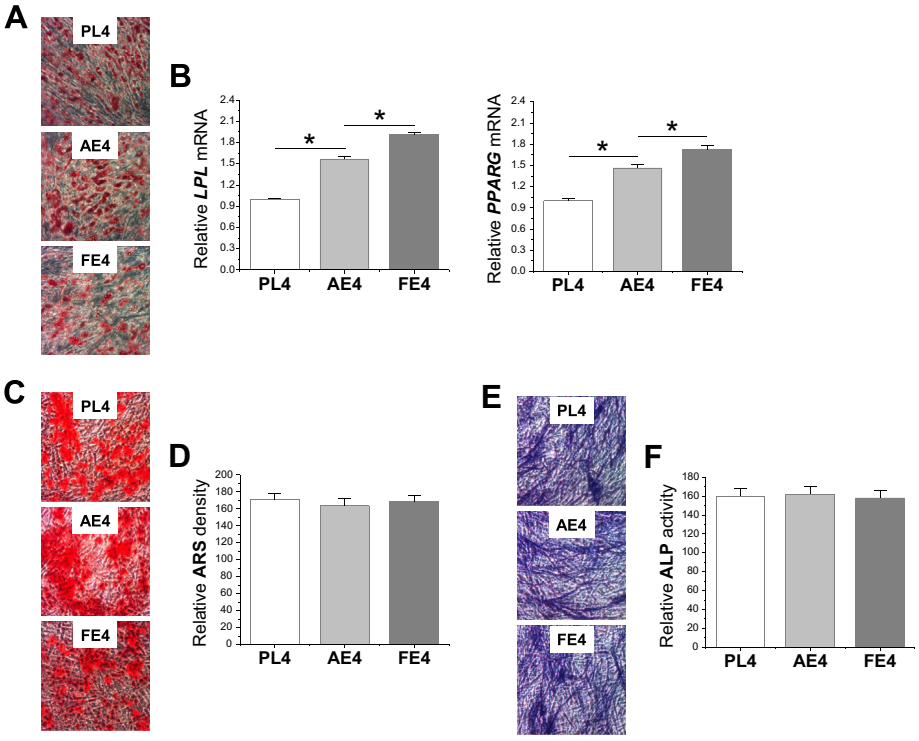

Fig 6 dECM pretreatment promoted expanded FSDSC adipogenesis rather than osteogenesis. After expansion on PL, AECM, or FECM, FSDSCs were replated in either adipogenic or osteogenic induction medium. After a 21-day incubation in adipogenic medium, adipogenesis was evaluated using Oil Red O staining (A) and quantitative adipogenic marker genes (*LPL* and *PPARG*) (B). After a 21-day incubation in osteogenic medium, osteogenesis was evaluated using Alizarin Red S (ARS) staining (C) and quantitative extracellular calcium assay (D) as well as alkaline phosphatase (ALP) staining (E) and quantitative activity assay (F). Data were shown as average ± SD for $n = 4$. *$p < 0.05$ indicated a statistically significant difference.

differentiation capacities after expansion on FECM and AECM. A possible explanation is that SDSCs are an adult stem cell inherently favoring chondrogenic and adipogenic differentiation rather than osteogenic differentiation.[4,5] dECM expansion augmented the inherent differentiation potential of a specific stem cell; for instance, dECM deposited by SDSCs favored expanded SDSCs' chondrogenic capacity[21] while dECM deposited by BMSCs benefited expanded BMSCs' endochondral bone formation.[22]

In conclusion, even though there is a history of fetal stem cell transplantation since 1928 and hundreds of clinical trials using various types of fetal transplants have been performed worldwide,[44] there are few studies investigating fetal stem cells from synovial tissue for chondrogenic potential. Different from adult stem cells with replicative senescence, in this study, we found that passaging human fetal SDSCs could yield enhanced chondrogenic capacity. Our study also suggests that a mature microenvironment can render fetal stem cells with lineage specific differentiation. The knowledge from this study will contribute to future cartilage regeneration and engineering using fetal source SDSCs in the treatment of osteoarthritic cartilage defects.

Competing interest statement

The authors report no conflict of interest.

Acknowledgments

The authors thank Suzanne Danley for her help in editing the manuscript, Dr. Sijin Wen for Biostatistical Consulting, and Vincent L. Kish for his help in biomechanical testing. This project was partially supported by Research Grants from the AO Foundation (S-12-19P) and National Institutes of Health (NIH) (no. 1 R03 AR062763-01A1).

References

1. Batty L, Dance S, Bajaj S, Cole BJ. Autologous chondrocyte implantation: an overview of technique and outcomes. *ANZ J Surg*. 2011;81:18—25.
2. Karnes J, Zhang Y, Pei M. Cell therapy for the creation of cartilage and related clinical trials. In: Templeton NS, ed. *Gene and Cell Therapy: Therapeutic Mechanisms and Strategies*. 4th ed. **2014. Boca Raton, FL, USA: Taylor & Francis/CRC Press; 2014:1123—1135.**
3. Steinert AF, Rackwitz L, Gilbert F, Nöth U, Tuan RS. Concise review: the clinical application of mesenchymal stem cells for musculoskeletal regeneration: current status and perspectives. *Stem Cells Transl Med*. 2012;1:237—247.
4. Jones B, Pei M. Synovium-derived stem cells: a tissue-specific stem cell for cartilage tissue engineering and regeneration. *Tissue Eng Part B Rev*. 2012;18:301—311.
5. Pizzute T, Lynch K, Pei M. Impact of tissue-specific stem cells on lineage specific differentiation: a focus on musculoskeletal system. *Stem Cell Rev*. 2015;11:119—132.

6. Li JT, Pei M. Cell senescence: a challenge in cartilage engineering and regeneration. *Tissue Eng Part B*. 2012;18:270—287.
7. Witkowska-Zimny M, Wrobel E. Perinatal sources of mesenchymal stem cells: Wharton's jelly, amnion and chorion. *Cell Mol Biol Lett*. 2011;16:493—514.
8. Clarkson ED. Fetal tissue transplantation for patients with Parkinson's disease: a database of published clinical results. *Drugs Aging*. 2001;18:773—785.
9. Hohlfeld J, de Buys Roessingh A, Hirt-Burri N, et al. Tissue engineered fetal skin constructs for paediatric burns. *Lancet*. 2005;366:840—842.
10. Rosser AE, Barker RA, Armstrong RJ, et al. Staging and preparation of human fetal striatal tissue for neural transplantation in Huntington's disease. *Cell Transpl*. 2003;12:679—686.
11. Touraine JL. In utero fetal liver cell transplantation in the treatment of immunodeficient or thalassemic human fetuses. *Transfus Sci*. 1993;14:299—304.
12. Le Blanc K, Götherström C, Ringdén O, et al. Fetal mesenchymal stem-cell engraftment in bone after in utero transplantation in a patient with severe osteogenesis imperfecta. *Transplantation*. 2005;79:1607—1614.
13. O'Donoghue K, Fisk NM. Fetal stem cells. *Best Pract Res Clin Obstet Gynaecol*. 2004;18:853—875.
14. Frost J, Monk D, Moschidou D, et al. The effects of culture on genomic imprinting profiles in human embryonic and fetal mesenchymal stem cells. *Epigenetics*. 2011;6:52—62.
15. Zhang ZY, Teoh SH, Hui JH, Fisk NM, Choolani M, Chan JK. The potential of human fetal mesenchymal stem cells for off-the-shelf bone tissue engineering application. *Biomaterials*. 2012;33:2656—2672.
16. Li JT, He F, Pei M. Creation of an in vitro microenvironment to enhance human fetal synovium-derived stem cell chondrogenesis. *Cell Tissue Res*. 2011;345:357—365.
17. Li JT, Hansen K, Zhang Y, et al. Rejuvenation of chondrogenic potential by young stem cell microenvironment. *Biomaterials*. 2014;35:642—653.
18. Pei M, Zhang Y, Li J, Chen D. Antioxidation of decellularized stem cell matrix promotes human synovium-derived stem cell-based chondrogenesis. *Stem Cells Dev*. 2013;22:889—900.
19. Rodriguez F, Patel SK, Cohen C. Measuring the modulus of a sphere by squeezing between parallel plates. *J Appl Polym Sci*. 1990;40:285—295.
20. Toh WS, Foldager CB, Pei M, Hui JH. Advances in mesenchymal stem cell-based strategies for cartilage repair and regeneration. *Stem Cell Rev*. 2014;10:686—696.
21. He F, Chen XD, Pei M. Reconstruction of an in vitro tissue-specific microenvironment to rejuvenate synovium-derived stem cells for cartilage tissue engineering. *Tissue Eng Part A*. 2009;15:3809—3821.
22. Pei M, He F, Kish VL. Expansion on extracellular matrix deposited by human bone marrow stromal cells facilitates stem cell proliferation and tissue-specific lineage potential. *Tissue Eng Part A*. 2011;17:3067—3076.
23. Pei M, Li JT, Zhang Y, Liu G, Wei L, Zhang Y. Expansion on matrix deposited by nonchondrogenic urine stem cells strengthens repeated passage bone marrow stromal cells' chondrogenic capacity. *Cell Tissue Res*. 2014;356:391—403.
24. Guillot PV, Gotherstrom C, Chan J, Kurata H, Fisk NM. Human first-trimester fetal MSC express pluripotency markers and grow faster and have longer telomeres than adult MSC. *Stem Cells*. 2007;25:646—654.
25. He F, Pei M. Extracellular matrix enhances differentiation of adipose stem cells from infrapatellar fat pad toward chondrogenesis. *J Tissue Eng Regen Med*. 2013;7:73—84.
26. Li JT, Pei M. Optimization of an in vitro three-dimensional microenvironment to reprogram synovium-derived stem cells for cartilage tissue engineering. *Tissue Eng Part A*. 2011;17:703—712.
27. Pei M, He F, Wei L. Three dimensional cell expansion substrate for cartilage tissue engineering and regeneration: a comparison in decellularized matrix deposited by synovium-derived stem cells and chondrocytes. *J Tissue Sci Eng*. 2011;2:104.
28. He F, Pei M. Rejuvenation of nucleus pulposus cells using extracellular matrix deposited by synovium-derived stem cells. *Spine*. 2012;37:459—469.
29. Pei M, He F. Extracellular matrix deposited by synovium-derived stem cells delays chondrocyte dedifferentiation and enhances redifferentiation. *J Cell Physiol*. 2012;227:2163—2174.
30. Pei M, Shoukry M, Li JT, Daffner SD, France JC, Emery SE. Modulation of in vitro microenvironment facilitates synovium-derived stem cell-based nucleus pulposus tissue regeneration. *Spine*. 2012;37:1538—1547.
31. Ng CP, Sharif AR, Heath DE, et al. Enhanced ex vivo expansion of adult mesenchymal stem cells by fetal mesenchymal stem cell ECM. *Biomaterials*. 2014;35:4046—4057.
32. Brady K, Dickinson SC, Guillot PV, et al. Human fetal and adult bone marrow-derived mesenchymal stem cells use different signaling pathways for the initiation of chondrogenesis. *Stem Cells Dev*. 2014;23:541—554.
33. Lynch K, Pei M. Age associated communication between cells and matrix: a potential impact on stem cell-based tissue regeneration strategies. *Organogenesis*. 2014;10:289—298.
34. Choi HR, Cho KA, Kang HT, et al. Restoration of senescent human diploid fibroblasts by modulation of the extracellular matrix. *Aging Cell*. 2011;10:148—157.
35. Szalai E, Felszeghy S, Hegyi Z, Módis Jr L, Berta A, Kaarniranta K. Fibrillin-2, tenascin-C, matrilin-2, and matrilin-4 are strongly expressed in the epithelium of human granular and lattice type I corneal dystrophies. *Mol Vis*. 2012;18:1927—1936.
36. Brinckmann J, Hunzelmann N, Kahle B, et al. Enhanced fibrillin-2 expression is a general feature of wound healing and sclerosis: potential alteration of cell attachment and storage of TGF-beta. *Lab Invest*. 2010;90:739—752.
37. Olivieri J, Smaldone S, Ramirez F. Fibrillin assemblies: extracellular determinants of tissue formation and fibrosis. *Fibrogenes Tissue Repair*. 2010;3:24.
38. Udalova IA, Ruhmann M, Thomson SJ, Midwood KS. Expression and immune function of tenascin-C. *Crit Rev Immunol*. 2011;31:115—145.
39. Ward M, Ajuwon KM. Regulation of pre-adipocyte proliferation and apoptosis by the small leucine-rich proteoglycans, biglycan and decorin. *Cell Prolif*. 2011;44:343—351.
40. Derfoul A, Perkins GL, Hall DJ, Tuan RS. Glucocorticoids promote chondrogenic differentiation of adult human mesenchymal stem cells by enhancing expression of cartilage extracellular matrix genes. *Stem Cells*. 2006;24:1487—1495.
41. Tallheden T, Karlsson C, Brunner A, et al. Gene expression during redifferentiation of human articular chondrocytes. *Osteoarthr Cartil*. 2004;12:525—535.
42. Serra R, Chang C. TGF-beta signaling in human skeletal and patterning disorders. *Birth Defects Res C Embryo Today*. 2003;69:333—351.
43. Kaur S, Soto-Pantoja DR, Stein EV, et al. Thrombospondin-1 signaling through CD47 inhibits self-renewal by regulating c-Myc and other stem cell transcription factors. *Sci Rep*. 2013;3:1673.
44. Ishii T, Eto K. Fetal stem cell transplantation: past, present, and future. *World J Stem Cells*. 2014;6:404—420.